Article

Optical properties of a fabricated self-assembled bottom-up bulk metamaterial

MÜHLIG, S., *et al*.

Abstract

We investigate the optical properties of a true three-dimensional metamaterial that was fabricated using a self-assembly bottom-up technology. The metamaterial consists of closely packed spherical clusters being formed by a large number of non-touching gold nanoparticles. After presenting experimental results, we apply a generalized Mie theory to analyze its spectral response revealing that it is dominated by a magnetic dipole contribution. By using an effective medium theory we show that the fabricated metamaterial exhibits a dispersive effective permeability, i.e. artificial magnetism. Although this metamaterial is not yet left-handed it might serve as a starting point for achieving bulk metamaterials by using bottom-up approaches.

Reference

MÜHLIG, S., *et al*. Optical properties of a fabricated self-assembled bottom-up bulk metamaterial. *Optics Express*, 2011, vol. 19, no. 10, p. 9607-9616

DOI : 10.1364/OE.19.009607

Optical properties of a fabricated self-assembled bottom-up bulk metamaterial

S. Mühlig,[1,*] C. Rockstuhl,[1] V. Yannopapas,[2] T. Bürgi,[3] N. Shalkevich,[4] and F. Lederer[1]

[1] *Institute of Condensed Matter Theory and Solid State Optics, Abbe Center of Photonics, Friedrich-Schiller-Universität Jena, Max-Wien-Platz 1, 07743 Jena, Germany*

[2] *Department of Materials Science, University of Patras, GR-26504 Patras, Greece*

[3] *Département de Chimie Physique, Université de Genève, Quai Ernest-Ansermet 30, 1211 Genève, Switzerland*

[4] *Institute of Physics ,University of Neuchatel, Rue Emile-Argand 11, 2009 Neuchatel, Switzerland*

[*] *stefan.muehlig@uni-jena.de*

Abstract: We investigate the optical properties of a true three-dimensional metamaterial that was fabricated using a self-assembly bottom-up technology. The metamaterial consists of closely packed spherical clusters being formed by a large number of non-touching gold nanoparticles. After presenting experimental results, we apply a generalized Mie theory to analyze its spectral response revealing that it is dominated by a magnetic dipole contribution. By using an effective medium theory we show that the fabricated metamaterial exhibits a dispersive effective permeability, i.e. artificial magnetism. Although this metamaterial is not yet left-handed it might serve as a starting point for achieving bulk metamaterials by using bottom-up approaches.

OCIS codes: (160.3918) Metamaterials; (160.4760) Optical properties; (250.5403) Plasmonics; (290.4210) Multiple scattering.

References and links

1. S. Zhang, W. Fan, N. C. Panoiu, K. J. Malloy, R. M. Osgood, and S. R. J. Brueck, "Experimental demonstration of near-infrared negative-index metamaterials," Phys. Rev. Lett. **95**, 137404 (2005).
2. N. Liu, H. Guo, L. Fu, S. Kaiser, H. Schweizer, and H. Giessen, "Three-dimensional photonic metamaterials at optical frequencies," Nature Mater. **7**, 31–37 (2008).
3. T. Paul, C. Rockstuhl, C. Menzel, and F. Lederer, "Anomalous refraction, diffraction, and imaging in metamaterials," Phys. Rev. B **79**, 115430 (2009).
4. D. A. Pawlak, S. Turczynski, M. Gajc, K. Kolodziejak, R. Diduszko, K. Rozniatowski, J. Smalc, and I. Vendik, "How far are we from making metamaterials by self-organization? The microstructure of highly anisotropic particles with a SRR-like geometry," Adv. Funct. Mater. **20**, 1116–1124 (2010).
5. J. A. Fan, C. Wu, K. Bao, J. Bao, R. Bardhan, N. J. Halas, V. N. Manoharan, P. Nordlander, G. Shvets, and F. Capasso, "Self-assembled plasmonic nanoparticle clusters," Science **328**, 1135–1138 (2010).
6. C. Menzel, T. Paul, C. Rockstuhl, T. Pertsch, S. Tretyakov, and F. Lederer, "Validity of effective material parameters for optical fishnet metamaterials," Phys. Rev. B **81**, 035320 (2010).
7. C. Rockstuhl, F. Lederer, C. Etrich, T. Pertsch, and T. Scharf, "Design of an artificial three-dimensional composite metamaterial with magnetic resonances in the visible range of the electromagnetic spectrum," Phys. Rev. Lett. **99**, 017401 (2007).
8. C. R. Simovski and S. A. Tretyakov, "Model of isotropic resonant magnetism in the visible range based on core-shell clusters," Phys. Rev. B **79**, 045111 (2009).

#142178 - $15.00 USD Received 8 Feb 2011; revised 25 Mar 2011; accepted 4 Apr 2011; published 3 May 2011

9. A. Vallecchi, M. Albani, and F. Capolino,"Collective electric and magnetic plasmonic resonances in spherical nanoclusters," Opt. Express **19**, 2754–2772 (2011).
10. V. Yannopapas, "Subwavelength imaging of light by arrays of metal-coated semiconductor nanoparticles: a theoretical study," J. Phys.: Condens. Matter **20**, 255201 (2008).
11. V. Yannopapas and A. Moroz, "Negative refractive index metamaterials from inherently non-magnetic materials for deep infrared to terahertz frequency ranges," J. Phys.: Condens. Matter **17**, 3717–3734 (2005).
12. M. S. Wheeler, J. S. Aitchison, J. I. L. Chen, G. A. Ozin, and M. Mojahedi, "Infrared magnetic response in a random silicon carbide micropowder," Phys. Rev. B **79**, 073103 (2009).
13. V. Yannopapas, "Artificial magnetism and negative refractive index in three-dimensional metamaterials of spherical particles at near-infrared and visible frequencies," Appl. Phys. A **87**, 259-264 (2007).
14. V. A. Tamma, J.-H. Lee, Q. Wu, and W. Park, "Visible frequency magnetic activity in silver nanocluster metamaterial," Appl. Opt. **49**, A11–A17 (2010).
15. J. Bang, U. Jeong, D. Y. Ryu, T. P. Russell, and C. J. Hawker, "Block copolymer nanolithography: translation of molecular level control to nanoscale patterns," Adv. Mater. **21**, 4769–4792 (2009).
16. H. Fan, "Nanocrystal-micelle: synthesis, self-assembly and application," Chem. Commun., 1383-1394 (2008).
17. S. Frein, J. Boudon, M. Vonlanthen, T. Scharf, J. Barberá, G. Süss-Fink, T. Bürgi, and R. Deschenaux, "Liquid-crystalline thiol- and disulfide-based dendrimers for the functionalization of gold nanoparticles," Helv. Chim. Acta **91**, 2321–2337 (2008).
18. P. W. K. Rothemund, "Folding DNA to create nanoscale shapes and patterns," Nature **440**, 297–302 (2006).
19. C. Helgert, C. Rockstuhl, C. Etrich, C. Menzel, E.-B. Kley, A. Tünnermann, F. Lederer, and T. Pertsch, "Effective properties of amorphous metamaterials," Phys. Rev. B **79**, 233107 (2009).
20. V. Yannopapas, "Negative refraction in random photonic alloys of polaritonic and plasmonic microspheres," Phys. Rev. B **75**, 035112 (2007).
21. N. Shalkevich, A. Shalkevich, L. Si-Ahmed, and T. Bürgi, "Reversible formation of gold nanoparticle–surfactant composite assemblies for the preparation of concentrated colloidal solutions," Phys. Chem. Chem. Phys. **11**, 10175–10179 (2009).
22. G. Frens, "Controlled nucleation for the regulation of the particle size in monodisperse gold suspensions," Nature (London), Phys. Sci. **241**, 20–22 (1973).
23. Y.-l. Xu, "Electromagnetic scattering by an aggregate of spheres," Appl. Opt. **34**, 4573–4588 (1995).
24. S. Mühlig, C. Rockstuhl, J. Pniewski, C. R. Simovski, S. A. Tretyakov, and F. Lederer, "Three–dimensional metamaterial nanotips," Phys. Rev. B **81**, 075317 (2010).
25. P. B. Johnson and R. W. Christy, "Optical constants of the noble metals," Phys. Rev. B **6**, 4370–4379 (1972).
26. T. Okamoto, "Near-field spectral analysis of metallic beads," in *Near-Field Optics and Surface Plasmon Polaritons*, S. Kawata, ed. (Springer, 2001), pp. 97–123.
27. L. A. Sweatlock, S. A. Maier, H. A. Atwater, J. J. Penninkhof, and A. Polman, "Highly confined electromagnetic fields in arrays of strongly coupled Ag nanoparticles," Phys. Rev. B **71**, 235408 (2005).
28. J. D. Jackson, "Radiating systems, multipole fields and radiation," in *Classical Electrodynamics*, 3rd ed. (Wiley, 1999), pp. 407–455.
29. C. Menzel, C. Rockstuhl, T. Paul, F. Lederer, and T. Pertsch, "Retrieving effective parameters for metamaterials at oblique incidence," Phys. Rev. B **77**, 195328 (2008).
30. H. Yan, S. I. Lim, Y.-J. Zhang, Q. Chen, D. Mott, W.-T. Wu, D.-L. An, S. Zhou, and C.-J. Zhong, "Molecularly-mediated assembly of gold nanoparticles with interparticle rigid, conjugated and shaped aryl ethynyl structures," Chem. Commun. **46**, 2218–2220 (2010).

1. Introduction

During the last decade much effort has been devoted to theoretically and experimentally investigate metamaterials (MMs). Generally, MMs consist of resonant unit cells, sometimes termed meta-atoms, considerably smaller than the wavelength. Most, if not to say all, MMs are currently fabricated by top-down technologies, such as e.g., electron or focused ion beam lithography. By using these technologies, however, the manufactured MMs are essentially planar having a negligible extension into the third dimension [1]. A sequential repetition of such a technology can partially overcome this restriction and may permit the fabrication of thicker MMs [2]. To date, apart from these options, it is difficult to get true bulk MMs by top-down technologies required for exploiting the peculiarities of light propagation in MMs [3]. MMs fabricated by top-down technologies have usually two peculiarities: they are periodic, constituting thus a perfect deterministic system, and the meta-atoms can be arbitrarily closely spaced leading to a high filling fraction.

#142178 - $15.00 USD Received 8 Feb 2011; revised 25 Mar 2011; accepted 4 Apr 2011; published 3 May 2011

Bottom-up self-assembly technologies are an alternative approach to fabricate MMs. Although such MMs usually consist of amorphously arranged meta-atoms and exhibit a smaller filling fraction, they are promising candidates because of their potential 3D extension as demonstrated for split-ring resonators [4]. Alternatively, clusters of spheres were also recently fabricated by related technologies [5]. Moreover, bottom-up MMs can potentially circumvent problems that are related to the strict periodic arrangement of meta-atoms, such as, e.g., the strong spatial dispersion [6]. First steps to fabricate some specific designs have already been reported, but the assignment of effective properties to fabricated structures and the simulation of the measured spectra (and therefore the physical understanding of these structures) is largely missing [4]. Up to now most simulation tools are restricted to top-down MMs which consist of periodically arranged identical meta-atoms. Generally, this requirement can be hardly met by self-assembly technologies.

One of the most promising approaches for the bottom-up fabrication of MMs consists in a suitable arrangement of metallic nanoparticles (NPs). Concepts like the meta-meta-material [7] or the core-shell system [8–10] exploit the scattering response of a cluster of spherical metallic NPs exhibiting a strong magnetic dipole moment. There are different explanations for this effect; one of them is based on the excitation of localized surface plasmons (LSPs) in metallic NPs forming a composite medium that then exhibits a large dispersive effective permittivity in the respective spectral range. Now, a sphere fabricated from that composite material represents a meta-atom and may possess a strong Mie resonance at a wavelength slightly larger than the LSP resonance. The lowest order Mie resonance is associated with a magnetic dipole [11–14]. Thus, an amorphous spatial arrangement of such spherical clusters (meta-atoms) can evoke a dispersive, but isotropic effective permeability or in other words artificial magnetism.

To fabricate such MMs, various chemical or biological processes can be exploited. Self-assembly can be induced by, e.g, blockcopolymers [15, 16], dentritic molecules [17] or DNA origami [18]. The incorporation of resonant NPs into these structures allows fabricating a MM. Most of these processes are required to show at least a self-assembly over volumes that are necessary to form individual meta-atoms. Long range order along various meta-atoms, as achieved by top-down technologies, is hard to realize with most of the bottom-up approaches. Therefore, only resonances that arise from the meta-atoms itself rather than from their periodic arrangement are required in most of the self-assembled bottom-up MMs. Fortunately, it has been shown that artificial magnetism persists even in fully disordered (amorphous) MMs [19, 20]. Therefore, it suffices to analyze the scattering properties of the meta-atoms rather than them of the complete self-assembled MM.

In this work we will provide such an analysis and link the spectral properties measured for a fabricated self-assembled bottom-up MM to its effective properties.

To begin with we provide some technical information on the fabrication of this specific MM, detail its geometry, and present the respective measured UV-VIS extinction spectra. This section is kept rather concise since more details can be found elsewhere [21]. Then we proceed in theoretically investigating the fabricated structures. Specifically we relate the resonances in the measured spectra to a resonance of the magnetic dipole moment. The effective parameters of an amorphous arrangement of such meta-atoms can be extracted leading to a dispersive effective permeability. By excluding alternative effects that could potentially explain the measured spectra, we will conclude that the fabricated structure represents a true three-dimensional MM with an isotropic magnetic response in the visible and near-infrared spectral domain. Our approach is versatile and can be used analyzing any MM fabricated by similar techniques.

#142178 - $15.00 USD Received 8 Feb 2011; revised 25 Mar 2011; accepted 4 Apr 2011; published 3 May 2011

2. Fabrication and experimental characterization

The MM studied here is fabricated by a two-step procedure. At first, gold NPs (that exhibit a nearly spherical shape) are synthesized using the Turkevich-Frens method [22]. Highly stable gold NPs, which are capped by sodium citrate that prevents them from touching, can be achieved by this procedure in an aqueous medium. Later the meta-atoms (clusters) are fabricated from these NPs of either 17 or 40 nm diameter. The choice of these diameters is arbitrary since the optical features of the structures under study are more or less independent of the NP size.

At second, a thiol ligand, namely the triethyleneglycolmono-11-mercaptoundecylether (EGMUDE) molecule replaces the sodium citrate at the NPs surface. Depending on the time, a self-assembly process is initiated that consists of three distinct stages [21].

Directly after adding the EGMUDE molecule (this is the first stage) the gold NPs start agglomerating where adjacent ones are almost touching. In the second stage (approximately $5-10$ minutes after EGMUDE addition) these agglomerates decay and supramolecular clusters are formed as can be seen in Fig. 1 (a) and (b). The gold NPs are clearly separated although their interparticle distance is less than twice the length of the EGMUDE molecule (which is ≈ 5.5 nm) . At the beginning the diameter of the supramolecular clusters amounts to about 1 μm (for 17 nm gold NPs) and becomes smaller in the following time which has been proven by dynamic light scattering in Ref. [21]. In the third stage (approximately 24 h after EGMUDE addition for 17 nm gold NPs) the supramolecular clusters dissolve (no explicit outer shape can be observed) and clearly ordered phases are observed as can be seen in Fig. 1 (c). There the distance between the particles corresponds to twice the length of the EGMUDE molecule as it was mentioned in Ref. [21], in other words all NPs should be fully covered by EGMUDE at this stage. It has to be stressed that the supramolecular clusters, whose optical properties are in the focus of interest in this contribution, are only temporarily stable since they dissolve themselves in the third stage. However, there is sufficient time left to evaluate their optical properties. Interestingly, the structures observed in the third stage exhibit on the one side long-term stability [21] but on the other side no interesting optical properties as can be seen later.

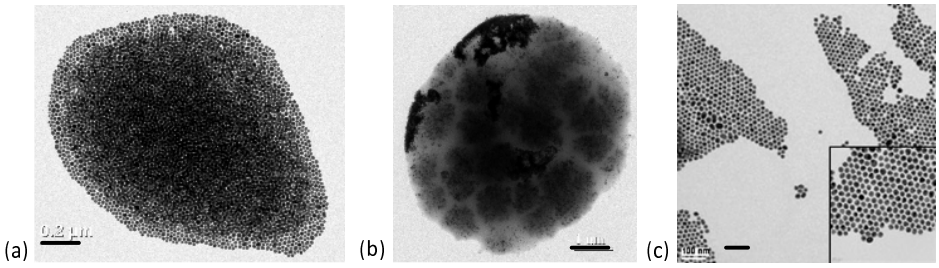

Fig. 1. Transmission electron micrographs of self-assembled gold nanoparticles with 17 nm diameter at different instants after having added the EGMUDE molecule [21]. (a), (b) 10 minutes and (c) 7 days after EGMUDE addition. In (a) a single supramolecular cluster can be seen (the black bar indicates 200 nm) whereas in (b) an arrangement of clusters is shown (the black bar indicates 1 μm). Panel (c) depicts the clearly ordered phase where the supramolecular clusters are dissolved (the black bar indicates 100 nm). Partly adapted from [21]. Reproduced by permission of the PCCP Owner Societies.

The measured UV-VIS extinction spectra of the fabricated samples in solution at representative instants are shown in Fig. 2 [21]. Both gold NPs with a diameter of 17 and 40 nm without EGMUDE addition exhibit a LSP resonance at 526 and 531 nm, respectively. After adding the EGMUDE and functionalizing the NPs with it, an additional red-shifted resonance appears.

#142178 - $15.00 USD Received 8 Feb 2011; revised 25 Mar 2011; accepted 4 Apr 2011; published 3 May 2011

Because the widths of both resonances (the LSP resonance and the additional one) are quite broad one cannot clearly separate them. It is evident that the additional red-shifted resonance stems from the supramolecular clusters. Because in the measured solution both NPs and clusters are present there are these two distinct resonances. The spectral separation between both resonances depends on the NP size and the elapsed time after EGMUDE was added. After the self-assembly process described above, the cluster dissolved after 24 h for 17 nm NPs and 3 days for 40 nm NPs. This is confirmed by the complete disappearance of the red-shifted cluster resonance [21]. By properly analyzing the spectral properties the above clusters we show below that the scattered field applying to this red-shifted cluster resonance is mainly due to a resonant magnetic dipole moment. This will lead to a strongly dispersive effective permeability of a MM formed by these supramolecular clusters [see Fig. 1 (b)].

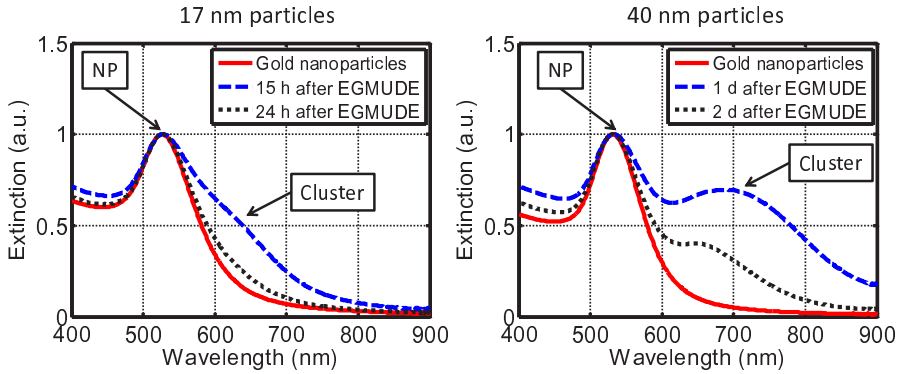

Fig. 2. Measured UV-VIS extinction spectra for gold NPs in solution (left panel: 17 nm diameter; right panel: 40 nm diameter) before (red solid graph) and at different instants after EGMUDE addition [21]. The black arrows designate distinct resonances measured in solution; the resonance labeled by "NP" corresponds to the LSP resonance of single NPs whereas the resonance labeled by "Cluster" corresponds to the resonance that is evoked by the supramolecular clusters [see Fig. 1 (a)].

3. Optical properties

In our theoretical work we rely on the analytical solution of Maxwell's equations for particles with a spherical symmetry, well-known as Mie theory, that was extended to handle aggregates of spheres [23, 24]. Thus we can calculate all quantities of interest for clusters consisting of arbitrarily arranged NPs with a spherical shape; as they appear in the experiments (see Fig. 1).

As can be seen in Fig. 1 (a) the gold NPs form supramolecular clusters with an almost spherical shape. The cluster geometry affects its optical response and evokes the additional resonance that is red-shifted compared to the LSP resonance (see black arrows in Fig. 2). As we are only interested in this resonance, we can restrict ourselves to simulating spherical clusters consisting of amorphous arranged spherical gold NPs. Material parameters were taken from Ref. [25] with a size-dependent correction for the imaginary part [26]. The clusters are illuminated by a plane wave propagating along the z direction with a polarization of the electric field parallel to the x direction. Since Mie theory holds in frequency domain every dot forming the extinction spectra in Fig. 3 corresponds to a simulation of the optical response. All series expansions of physical quantities as they appear in Mie theory [23, 24] were considered up to the fifth order (we observe no changes in the simulated spectra when comparing these results with simulations up to the sixth order). The only constraint we imposed was a minimal distance between

#142178 - $15.00 USD Received 8 Feb 2011; revised 25 Mar 2011; accepted 4 Apr 2011; published 3 May 2011

the NPs in the cluster, which was subject to changes. Thus this distance is a free parameter in the simulations and will serve later for fitting simulated and measured spectra. Furthermore, the introduced minimal distance prevents the NPs from touching. If the particles touch each other the plasmon resonance gets red-shifted, in other words the NPs are short-circuited and the response is dominated by an electron oscillation in a NP wire as it was shown in Ref. [27]. Thus touching NPs would not evoke the measured extinction spectra shown in Fig. 2 since in this case the resonance peak of a 1 μm cluster should appear in the far infrared (due to the large spatial extension of a scatterer that consists of connected gold NPs) and not in the visible spectral domain.

The cluster diameter is chosen to be eight times the NP diameter. This size guarantees reasonable CPU times using the available computational resources. To simulate larger cluster diameters we have to consider more spheres and therefore more memory is required to apply Mie theory; this limits the maximal number of spheres that can be investigated. Clusters consisting of up to ≈ 200 NPs were considered. The cluster diameter is about 5 times smaller than in the experiments. The impact of such a smaller diameter will be discussed below.

A sketch of one of the clusters considered in the simulations is displayed in the inset of Fig. 3. The permittivity ε of the surrounding medium is chosen such that the simulated NP LSP resonance wavelength coincides with the one measured in the experiments. This criterion is met for $\varepsilon = 1.73$ being very close to that of water. The slight deviation can be explained by the fact that the composition of the solvent is rather complex but dominated by water. The extinction cross-sections as a function of the wavelength and of the minimal distance between the NPs can be seen in Fig. 3. A remarkable red-shift of the cluster resonance with respect

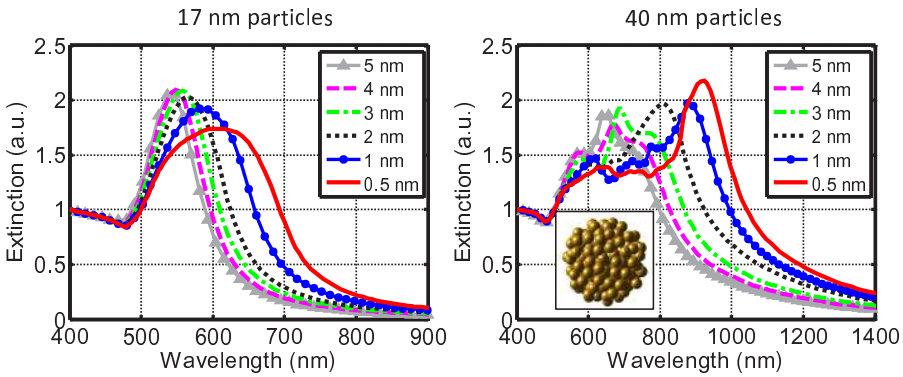

Fig. 3. Simulated extinction spectra of clusters with a spherical shape (the inset in the right panel depicts a sketch) made of gold NPs with different diameters (left panel: 17 nm; right panel 40 nm). The legend indicates the minimal distance between all the particles that form the cluster. Note that in contrast to the experimental spectra the single NP resonance is not shown here.

to the single NP resonance (not shown here) can be seen. It compares to that measured in the experiments (resonance labeled by “Cluster” Fig. 2) if the minimal distance between the NPs falls below 2 nm. It is crucial to note that the simulated spectra concern only a supramolecular cluster sketched in Fig. 3. The contribution of isolated NPs, which are not included in the self-assembling process but are still present in the solution, is disregarded. Therefore, the LSP resonance of these NPs at 526 nm and 531 nm for 17 nm and 40 nm NP diameters, respectively (as they appear in Fig. 2 labeled by ”NP”) are not reproduced by the simulations. In other words, the resonances in Fig. 3 has to be compared to those of Fig. 2 labeled by “Cluster”.

#142178 - $15.00 USD Received 8 Feb 2011; revised 25 Mar 2011; accepted 4 Apr 2011; published 3 May 2011

The simulated extinction spectra of the cluster of 40 nm NPs show some fine structure below the main resonance that is not observed in the measured extinction spectra (see Fig. 2). This fine structure arises due to the interparticle coupling of adjacent NPs. Therefore, it strongly depends on the precise spatial position of the NPs in the cluster. In the simulations only a single cluster is considered (as sketched in Fig. 3) whereas in the experiments there exists a huge number of clusters in solution. All these clusters in solution exhibit different spatial arrangements of NPs forming the cluster. Hence the fine structure could not be observed in the measured extinction spectra. Only the dominating red-shifted resonance could be observed since it is governed by the outer shape of the clusters. Furthermore, the width of the simulated red-shifted resonance is smaller when compared to the measured one. This is an effect of the slightly deviating outer shapes (from a perfect sphere) of the supramolecular clusters [see Fig. 1 (a), (b)]. Therefore, all extinction spectra of the single supramolecular clusters superimpose in the measured UV-visible spectra as shown in Fig. 2 and the red-shifted resonance appears broader compared to the simulations where only a single cluster is considered.

To be sure that the formation of such clusters is the appropriate explanation for the observed red-shifted cluster resonance, we double-checked our results in supporting simulations by simulating various alternative situations. First we considered mutual coupling between only two NPs. Such dimers exhibit significantly red-shifted resonances if the dipoles in both NPs oscillate in-phase along their connection line. We assume the same surrounding dielectric medium ($\varepsilon = 1.73$) and plane wave illumination as above. Two illumination directions (along the connection line and perpendicular to it) and two linear independent polarizations (parallel and perpendicular to the connection line) are considered and all results were superposed. In first approximation this procedure mimics an ensemble of randomly arranged dimers. The simulated extinction spectra in Fig. 4 clearly indicate that the experimentally observed red-shift is too large to be explained in terms of the mutual coupling of only two gold NPs. Even for very small distances of about 0.5 nm the simulation does not match the experimental results and the shift is always much smaller than observed.

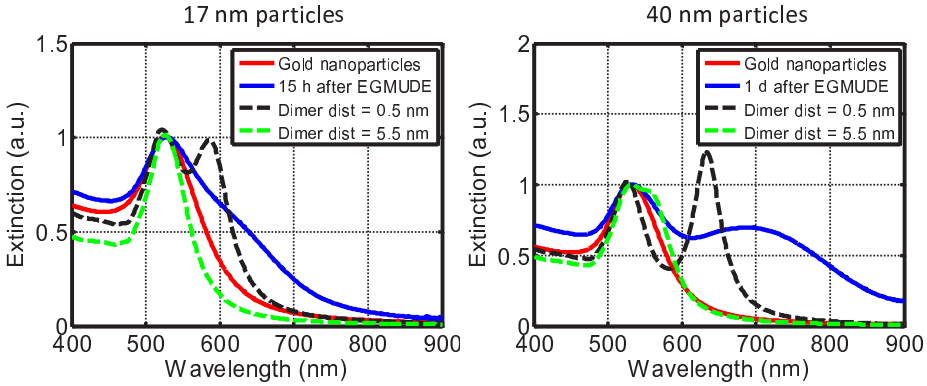

Fig. 4. Simulated extinction spectra for structures made of gold NPs with different diameters (left panel: 17 nm; right panel 40 nm). The solid lines show the measured results from Fig. 2 (the colorbar is maintained) and the dashed lines are related to randomly arranged dimers with two distinct NP separations.

As a second alternative we probed whether the coverage of gold NPs by an EGMUDE shell ($\varepsilon = 2.4$) can evoke the shift. It turns out, however, that the resonance of such a core-shell NP is red-shifted only by about 25 nm; even if the shell radius is four times larger than the core radius. This shift is too small to explain the experimental results. Furthermore, a different

#142178 - $15.00 USD Received 8 Feb 2011; revised 25 Mar 2011; accepted 4 Apr 2011; published 3 May 2011

dielectric permittivity of the surrounding medium would be no alternative explanation because the LSP resonance wavelength of the single gold NPs would no longer match the experimental results. To sum up our numerical investigations imply that the experimental spectra can be satisfactorily explained only by the self-assembled formation of supramolecular clusters from gold NPs upon adding EGMUDE molecules as observed in TEM.

In the following we aim at assigning effective material properties to a medium made of densely packed clusters. Prior to this we need to clarify an issue. The simulations have been carried out with the correct experimental data. There is only one exception. For the sake of saving a reasonable CPU time the simulated cluster size was less than in the experiment. However, this discrepancy can be compensated by a reduction of the minimum distance between NPs. This becomes evident by considering the red-shift as a function of these two geometrical cluster parameters. On the one hand, this shift reduces with the cluster diameter and on the other hand it increases with decreasing minimum NP separation (see also Fig. 3). By an appropriate choice of both geometrical parameters an almost complete compensation can be achieved at least up to cluster sizes eight times the NP size where this compensation effect was numerically studied in detail. Thus we can argue that it is possible to compensate the effect of simulating smaller clusters (compared to the experiments) by simultaneously choosing a smaller minimal distance between adjacent NPs. Therefore, although the quantitative value of the extracted geometrical parameters in the simulations need to be taken with care, the optical actions of both configurations should be comparable.

3.1. Unraveling artificial magnetism

As examined in Ref. [7] a sphere made of densely packed metallic NPs exhibits a strong, slightly red-shifted Mie resonance compared to the LSP resonance. This resonance is related to a magnetic dipole moment of the sphere. In these studies the NPs forming the sphere were periodically arranged; but it can be anticipated that disorder will only have a minor effect. Therefore, the relevance of a magnetic dipole (artificial magnetism) for the optical response of a cluster as shown in Fig. 3 can be evaluated by calculating the contributions of the individual multipole moments to the scattered field.

To retrieve the respective dipole moments Mie theory can be applied. There all fields, namely the incident, the scattered and the internal ones, are expanded into series of eigenfunctions. This expansion is, except for some prefactors, identical to a multipole expansion in spherical coordinates. By comparing this multipole expansion of the scattered field with the Cartesian one [28] one has direct access to the Cartesian multipoles. The cluster (for which the dipoles should be calculated) is excited by a linear polarized plane wave. To be specific, from now on we assume x-polarized light propagating along the z-direction. Only clusters formed by NPs with a minimal separation of 0.5 nm are considered in the following. The spectrally resolved components of both the electric and the magnetic dipole in Fig. 5 show that a resonance is predominantly induced in the magnetic dipole by the spherical shape of the clusters. The position of the magnetic dipole resonance coincides with the red-shifted extinction resonance in Fig. 3 (red solid graph). The magnetic dipole moment is induced along the y-direction, corresponding to the polarization of the incident magnetic field. This magnetic moment is much larger for larger NPs because of the larger cluster size (cluster diameter is eight times the NP diameter) in accordance with Mie theory. In Mie theory the scattering cross section is directly related to the multipole amplitudes [23]. Because an increasing cluster leads directly to an increasing scattering cross section (at a chosen wavelength) and consequently to larger multipole amplitudes which transform then naturally into the larger Cartesian multipole moments plotted in Fig. 5.

Besides the magnetic and the electric dipole moments, no higher order multipole moments are resonantly enhanced in the spectral domain of the red-shifted cluster resonance. Further-

#142178 - $15.00 USD Received 8 Feb 2011; revised 25 Mar 2011; accepted 4 Apr 2011; published 3 May 2011

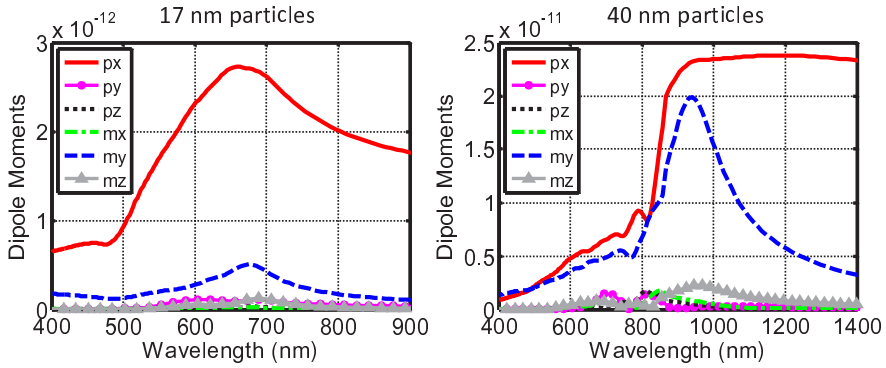

Fig. 5. Simulated dipole moments (p–electric; m–magnetic) for spherical clusters (identical to Fig. 3) made of gold NPs with two different diameters (left panel: 17 nm; right panel 40 nm). The structure is illuminated by a plane wave propagating along z-direction and an x-polarized electric field.

more, by comparing Fig. 5 with the calculated extinction spectra in Fig. 3 we can conclude that the red-shifted resonance as observed in both experiment and simulation is related to the magnetic dipole moment of the cluster. The decrease of all dipole moment components for shorter wavelengths in Fig. 5 is due to the increasing cluster size - wavelength ratio. The cluster size is no longer sub-wavelength and higher order multipole moments come into the play, sometimes dominating the optical response.

One common way for planar MMs to assign effective parameters is the inversion of reflection and transmission coefficients from a MM slab [29]. Here we want to introduce a different approach that should be more convenient for amorphous bulk MMs. We retrieve the effective properties of a MM made of an amorphous arrangement of supramolecular clusters [Fig. 1 (b)] and evaluate the strength of artificial magnetism by exploiting the well-known Clausius-Mossotti relation [28]. It links the local polarizability of the clusters to effective parameters as a function of the filling fraction. Here, the filling fraction was chosen to be 0.4 which is just an estimation motivated by TEM figures similar to Fig. 1 (b). There it can be seen that the supramolecular clusters tend to arrange in a rather dense package in solution. Thus a filling fraction of 0.4 is a reasonable choice for the structure studied here. The effective permeabilities are shown in Fig. 6 exhibiting a weak dispersion for 17 nm NPs diameters and a stronger one for 40 nm NPs.

Compared to theoretical results [7, 8] the artificial magnetism of our self-assembled real structure is less. This is not surprising because all imperfections enter this ultimate result. In contrast, the structures discussed in literature thus far are based on more or less simplified theoretical models. For example, all the previously examined structures rely on periodically arranged NPs. A well-defined long range order over large distances cannot be achieved with the exploited self-assembling bottom-up technique in Ref. [21]; this technique only allows to control the distance between adjacent NPs. The long range order upon arranging the NPs on a periodic lattice was shown to evoke a stronger dispersion in the effective properties [19]. Furthermore, in most of the previous simulations the NPs consisted of silver rather than gold. With silver being a better plasmonic material, the artificial dielectric and magnetic MM properties are expected to be more pronounced. And finally, a periodic arrangement allows to achieve NP filling fractions of up to 65 % compared to only about $30-40$ % in our amorphous structures

#142178 - $15.00 USD Received 8 Feb 2011; revised 25 Mar 2011; accepted 4 Apr 2011; published 3 May 2011

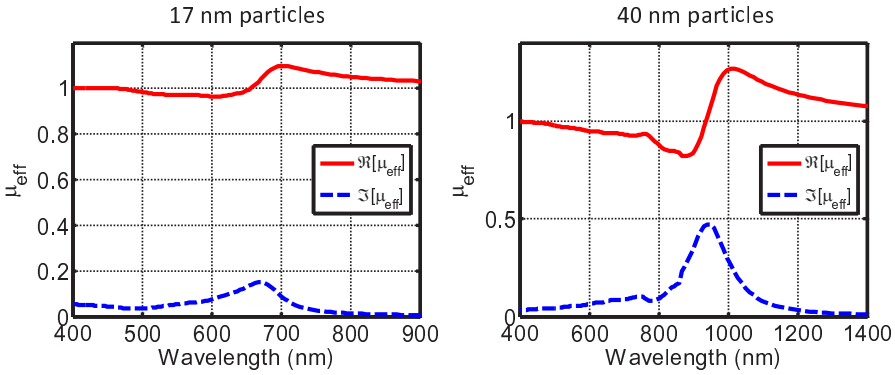

Fig. 6. Simulated effective permeability for clusters similar to Fig. 3 retrieved from the m_y dipole moment from Fig. 5.

4. Conclusions

The optical properties of a MM fabricated by using a self-assembly bottom-up technology were investigated. An explanation of the measured UV-VIS spectra was provided by rigorous simulations of the optical response of fabricated structures. Furthermore, we related the appearance of an additional red-shifted resonance to a magnetic dipole moment that is induced due to the spherical shape of the fabricated supramolecular clusters. By excluding other effects that could potentially explain the measured spectra we propose that the cluster supports an isotropic magnetic response in the visible regime. A dispersive effective permeability (artificial magnetism) was demonstrated using the Clausius-Mossotti relation. This Lorentzian resonance is, however, weaker when compared to previous theoretical predictions. We attribute this effect to the amorphous arrangement of nanospheres inside the cluster and worse plasmonic properties of gold compared to silver. The main disadvantage of the fabricated cluster structure is their dissolution after a certain time interval. This might be compensated by using other molecules as a ligand of the NPs to initiate the self-assembly. It has been proven [30] that conjugated and shaped aryl ethynyl structures can be used to fabricate long term stable spherical supramolecular gold clusters.

In addition to the study of this very structure, our work contributes to the assignment of effective properties to MMs fabricated by bottom-up self-assembly technologies. By departing from a qualified guess of the structural integrity of the MM (obtained by techniques such as TEM micrographs and dynamic light scattering) and measured extinction spectra from fabricated samples, we have shown that rigorous diffraction theory used to simulate the scattering response of an individual meta-atom (cluster) can be applied to understand the measured spectral features as e.g. additional resonances. These meta-atoms, as in our case, may exhibit complicated shapes and the simulations can be quite demanding. As a result we have shown that the scattered field of an individual meta-atom can be decomposed into contributions of electromagnetic multipoles. Using effective medium theories and taking advantage of the calculated multipole coeffcients the dispersive effective properties of MMs can be calculated.

Acknowledgments

Financial support by the Federal Ministry of Education and Research PHONA, from the State of Thuringia within the ProExcellence program MEMA, as well as from the European Union FP7 project NANOGOLD is acknowledged.

#142178 - $15.00 USD Received 8 Feb 2011; revised 25 Mar 2011; accepted 4 Apr 2011; published 3 May 2011